Inorganic Chemistry

Article

pubs.acs.org/IC

Dicobalt-μ-oxo Polyoxometalate Compound, $[(\alpha_2\text{-}P_2W_{17}O_{61}Co)_2O]^{14-}$: A Potent Species for Water Oxidation, C–H Bond Activation, and Oxygen Transfer

Delina Barats-Damatov,[†] Linda J. W. Shimon,[‡] Lev Weiner,[‡] Roy E. Schreiber,[†] Pablo Jiménez-Lozano,[§] Josep M. Poblet,[§] Coen de Graaf,[§,⊥] and Ronny Neumann*[,†]

[†]Department of Organic Chemistry, Weizmann Institute of Science, Rehovot, Israel, 76100

[‡]Chemical Research Support Unit, Weizmann Institute of Science, Rehovot, Israel, 76100

[§]Departament de Química Física i Inorgànica, Universitat Rovira i Virgili, 43007 Tarragona, Spain

[⊥]Institució Catalana de Recerca i Estudis Avançats (ICREA), Passeig Lluís Companys 23, 08010, Barcelona, Spain

Supporting Information

ABSTRACT: High-valent oxo compounds of transition metals are often implicated as active species in oxygenation of hydrocarbons through carbon–hydrogen bond activation or oxygen transfer and also in water oxidation. Recently, several examples of cobalt-catalyzed water oxidation have been reported, and cobalt(IV) species have been suggested as active intermediates. A reactive species, formally a dicobalt(IV)-μ-oxo polyoxometalate compound $[(\alpha_2\text{-}P_2W_{17}O_{61}Co)_2O]^{14-}$, $[(POMCo)_2O]$, has now been isolated and characterized by the oxidation of a monomeric $[\alpha_2\text{-}P_2W_{17}O_{61}Co^{II}(H_2O)]^{8-}$, $[POMCo^{II}H_2O]$, with ozone in water. The crystal structure shows a nearly linear Co–O–Co moiety with a Co–O bond length of ~1.77 Å. In aqueous solution $[(POMCo)_2O]$ was identified by ^{31}P NMR, Raman, and UV–vis spectroscopy. Reactivity studies showed that $[(POMCo)_2O]_2O]$ is an active compound for the oxidation of H_2O to O_2, direct oxygen transfer to water-soluble sulfoxides and phosphines, indirect epoxidation of alkenes via a Mn porphyrin, and the selective oxidation of alcohols by carbon–hydrogen bond activation. The latter appears to occur via a hydrogen atom transfer mechanism. Density functional and CASSCF calculations strongly indicate that the electronic structure of $[(POMCo)_2O]_2O]$ is best defined as a compound having two cobalt(III) atoms with two oxidized oxygen atoms.

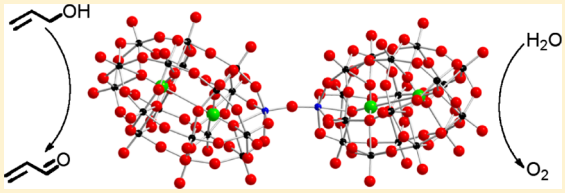

INTRODUCTION

In the biological world, the intermediacy of reactive oxo species of iron, copper, and manganese metalloenzymes enables C–H bond activation of hydrocarbons by monooxygenase enzymes[1] and water oxidation by photosystem II.[2] Beyond the importance of understanding the mode of activity of these metalloenzymes there is intense interest in the development of synthetic catalysts for such transformations. Thus, the oxidation of gaseous methane to liquid methanol would aid in the utilization of huge natural gas reserves,[3] and oxidation of water would enable formation of hydrogen gas as an alternative energy carrier.[4] Therefore, much research has been devoted to iron- and copper-based catalysts for hydrocarbon oxidation[5] and mostly ruthenium- and manganese-based catalysts, but also others for water oxidation.[6]

Cobalt salts and complexes have long been known to be active in hydrocarbon autoxidation reactions and for dioxygen coordination.[7] Their use in oxygen transfer reactions with oxygen donors that ostensibly form high-valent Co–O intermediates has been only relatively scantily investigated,[8] and it has been proposed that terminal Co^{IV}–oxo species may be formed and active.[9] Recently, such a Co^{IV}–oxo species stabilized by Sc^{3+} has been reported,[10] although others have suggested that this may be a $Co^{III}OH$ compound.[11] About 30 years ago, there were some reports on the use of aquo cobalt(II) for the oxidation of water to O_2 with Co^{IV} species suggested as active intermediates.[12] This general area of research has been revitalized after Kanan and Nocera's publication five years ago and subsequent research on the high activity of a cobalt-phosphate cluster for water oxidation.[13] Since then, there has been a flurry of activity where cobalt-containing compounds including molecular catalysts,[14] bio-inspired "cubane"-type compounds,[15] and various colloidal, cluster, and nanoparticulate materials[16] have been used for water oxidation. In this context, anionic cobalt-containing polyoxometalates have also been suggested as molecular water oxidation photocatalysts.[17] The stability of the catalysts under turnover conditions is being debated.[18]

Polyoxometalates also provide fascinating possibilities for the study of transition-metal reactivity with oxidants in a purely inorganic oxo-ligand environment and also in water.[19] They

Received: December 3, 2013
Published: January 17, 2014

   dx.doi.org/10.1021/ic402962c | Inorg. Chem. 2014, 53, 1779–1787

also allow stabilization of important intermediates otherwise not observable, as shown in the isolation of Fe(III)-peroxo species upon addition of O_2 to a hexasubstituted Fe(II) polyoxometalate.[20] Utilizing the intrinsic stability of polyoxometalate frameworks toward ozone, we have isolated a polyoxometalate-based dimer containing a *formally* Co^{IV}−O−Co^{IV} moiety. The isolation of this compound and its spectroscopic characterization has allowed us to demonstrate that it is a competent water oxidation species and is reactive for the selective C−H bond activation of water-soluble alcohols and oxygen transfer to sulfoxides. In the presence of a Mn(III) porphyrin, efficient oxygen transfer to alkenes was also demonstrated. Calculations show that the active compound is *not* a bis-Co^{IV} species, but rather it is better represented as a bis-Co^{III} compound with two oxygen-centered cation radicals or holes.

RESULTS AND DISCUSSION

Preparation and Characterization of Active Species. The experimental study was carried out using $[\alpha_2$-$P_2W_{17}O_{61}Co^{II}(H_2O)]^{8-}$ $[POMCo^{II}H_2O]$ with the Wells−Dawson structure as the polyoxoanion, Figure 1, and ozone

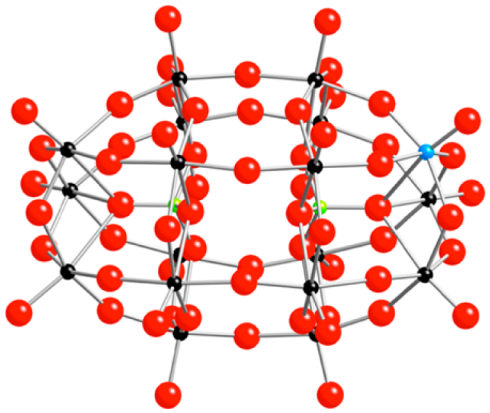

Figure 1. Ball and stick structural representation of $[POMCo^{II}H_2O]$. Solvent molecules and cations are not shown for clarity. P , green; W, black; O, red; Co, blue.

as oxidant. The rationale behind these choices was that ozone is a strong, potentially two-electron oxidant, known, by spectroscopic studies, to be able to form an Fe^{IV}═O species in water and thus was also a reasonable candidate for the formation of a Co^{IV} compound.[21] Furthermore, as has been shown in the past, polyoxometalates are typically water-soluble and stable toward ozone.[22] $[POMCo^{II}H_2O]$ has a specific advantage in that the two phosphorus atoms have different chemical environments, and this fact can effectively be utilized in ^{31}P NMR studies for speciation in solution.[23]

Thus, ozone (concentration 25 mg/L, rate 6.25 mg/min) dissolved in O_2 was bubbled through a 10 mM aqueous solution of $K_8[\alpha_2$-$P_2W_{17}O_{61}Co^{II}(H_2O)]^{8-}$, $K[POMCo^{II}H_2O]$, at ∼0 °C. After a few minutes the salmon pink solution began to turn dark red (maroon) and the ^{31}P NMR showed the formation of one new major species, Figure 2, left. The ^{31}P NMR spectrum of $K[POMCo^{II}H_2O]$, with a narrow peak at −25.6 ppm and a broad peak at +274.2 ppm, Figure 2, right, shows the typical behavior for the presence of a paramagnetic atom in the Wells−Dawson structure;[23] the upfield peak can be assigned to the phosphorus atom distal to Co^{II}, and the

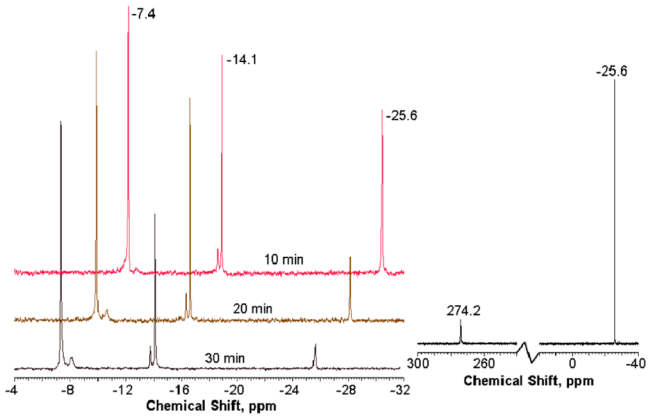

Figure 2. ^{31}P NMR spectrum of 10 mM aqueous $K[POMCo^{II}H_2O]$ at 22 °C (right) and changes upon ozonation as a function of time (left, where the peak at +274.2 ppm is not shown for convenience).

downfield peak can be assigned to the phosphorus atom vicinal to Co^{II}. The two peaks at −14.1 and −7.4 ppm that appeared upon ozonation are associated with the formation of $[(POMCo)_2O]$, as will be detailed below. After 30 min at 10 mM $K[POMCo^{II}H_2O]$ a conversion of 80−85% was measured. The appearance of a small, minor (∼5%) set of peaks at −8.1 and −13.8 ppm was also observed. These peaks are assigned to a one-electron-oxidized species $[POMCo^{III}H_2O]$ since treatment of $K[POMCo^{II}H_2O]$ with a one-electron oxidant such as $K_2S_2O_8$ yielded a spectrum with peaks at these chemical shifts, Figure S1. It is notable that after purging the ozonated solution with an inert gas within 1 h at room temperature the major peaks in the ^{31}P NMR spectrum associated with $[(POMCo)_2O]$ disappear with the reappearance of the peaks of the original $[POMCo^{II}H_2O]$ species. $[POMCo^{III}H_2O]$ was not formed during this reverse reaction. $[POMCo^{III}H_2O]$ was constant as a minor impurity and remained unchanged in the solution; it was stable for more than a week. There is no comproportionation of $[POMCo^{II}H_2O]$ and $[(POMCo)_2O]$ to $[POMCo^{III}H_2O]$.

The optical absorption spectrum of the ozonated and then Ar purged solution of $K[POMCo^{II}H_2O]$ is presented in Figure 3. At 150 μM one can easily see new absorption peaks at λ_3 = 381 nm, λ_4 = 507 nm. At a lower concentration of 12 μM the peaks in the UV region attributable to the ozonated species cannot be deconvoluted because of the strong charge transfer peak of the polyoxometalate framework. However, a difference

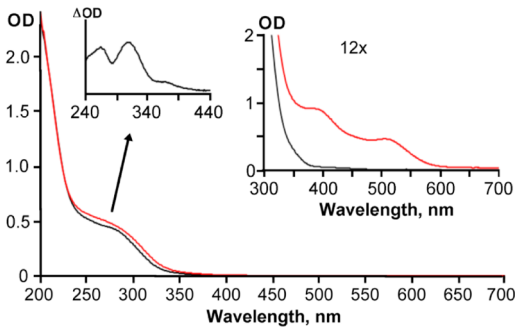

Figure 3. UV−vis spectra of 12 μM and 150 μM (right inset) aqueous solutions of $K[POMCo^{II}H_2O]$ at 22 °C (black line) and of an ozonated solution (red line) along with the difference spectrum for the UV range.

dx.doi.org/10.1021/ic402962c | *Inorg. Chem.* 2014, 53, 1779−1787

spectrum clearly revealed two additional peaks at λ_1 = 262 nm, λ_2 = 304 nm. Notably, [POMCo^{III}H$_2$O] has a very different UV−vis spectrum from that of [(POMCo)$_2$O], Figure S2.

Additional structural data on the ozonated species were obtained by Raman spectroscopy, Figure 4. The most notable

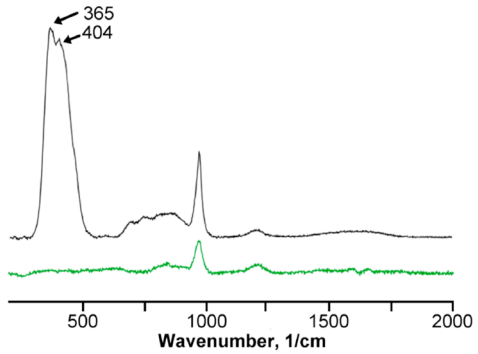

Figure 4. Raman spectrum of 10 mM aqueous solutions of K[POMCo^{II}H$_2$O] before (green) and after (black) ozonolysis.

feature is the appearance of the strong peaks at 365 and 404 cm^{-1}. These peaks can very reasonably be assigned to the symmetric Co−O−Co bond stretching vibrations, expected to be intense and in this very energy region due to the linearity of the bridging oxo ligand.[24] The asymmetric Co−O−Co bond stretching vibrations are expected at 800−900 cm^{-1}, but are weak.[24] Furthermore, for a linear Co−O−Co bond, no or only a small isotope effect is expected.[24] Indeed, the Raman spectrum is essentially unchanged when [(POMCo)$_2$O] was prepared in H$_2$^{18}O, though as will be shown below in the reactivity experiments, preparation of [(POMCo)$_2$O] in H$_2$^{18}O leads to an 18-O-labeled compound. Importantly, these vibrations can be observed in both the solid-state Raman and IR spectra, Figure S3, indicating that the same species are present in the solid state as well as in aqueous solution. Finally and also notable is the observation that the Raman spectrum of K[POMCo^{III}H$_2$O] is indistinguishable from that of K-[POMCo^{II}H$_2$O].

After numerous attempts over a period of two years, we were finally able to crystallize the product of the ozonation reaction, by addition of tetramethylammonium fluoride at ∼0 °C, followed by precipitation and recrystallization from a warm aqueous solution. Note that other available tetramethylammonium halides (Cl$^-$, Br$^-$) reacted immediately with the oxidized species. The compound is unstable under these conditions, *vide infra*, and the solution initially contains about 25−30% [POMCo^{II}H$_2$O] as measured by ^{31}P NMR. The crystallization needs to occur within 10−15 min before too much decay of [(POMCo)$_2$O] occurred, and only *very small*, 150 by 10 by 10 μm, needle-like crystals were formed. Despite this limitation and some disorder, the crystal structure as determined by single-crystal X-ray diffraction clearly indicates the formation of a Co−O−Co dimer species between two Wells−Dawson anions, Figure 5. Three diffraction measurements were made on different batches of crystals, and all showed this result. From the crystal structure Co−O$_{bridge}$ bond lengths of 1.79(3) and 1.77 (4) Å and a Co−O$_{bridge}$−Co bond angle of 167(2)° were determined. One may note that the best solution to the X-ray diffraction data indicates a partial occupancy of the Co atoms (90% and 77%). One explanation is that there are also Co−O−W bridged species. However, in such a situation, one would

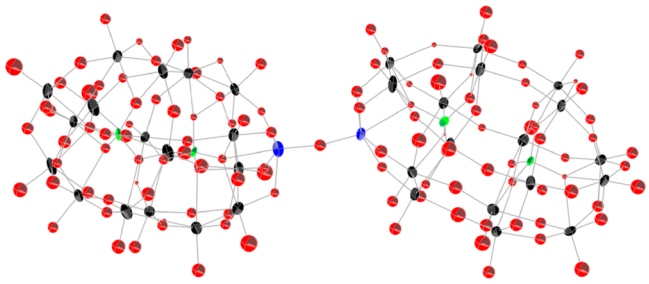

Figure 5. ORTEP structure (with 50% probability ellipsoids) of [(POMCo)$_2$O]. Solvent molecules and cations are not shown for clarity. P, green; W, black; O, red; Co, blue. Note: The Co occupancies are 90% and 77%; the remainder is refined as W.

expect to observe an indicative spectroscopic feature in the solution ^{31}P NMR. Another more likely explanation is that the [(POMCo)$_2$O] compound cocrystallizes with [POMCo^{II}H$_2$O], present as an impurity. Indeed, the MAS ^{31}P NMR spectrum of crystalline [(POMCo)$_2$O], Figure S4, shows the presence of the [POMCo^{II}H$_2$O] as an impurity. Since [POMCo^{II}H$_2$O] does not crystallize anisotropically, there is likely some disorder at all positions; it is more observable at the unique cobalt positions since some W at a Co position has a much larger effect than some Co at a W position. The countercations in the structure (Me$_4$N$^+$ and K$^+$) are partially disordered and could not be well refined.

Direct measurement of the oxidation state of the cobalt atom proved to be impossible. X-ray photon spectroscopy (XPS) measurements, Figure S5, carried out on [POMCo^{II}H$_2$O], [POMCo^{III}H$_2$O], and [{(POMCo)$_2$O] clearly showed a higher binding energy for Co^{III} versus Co^{II}, as would be expected; however the reducing conditions of the XPS measurements, as was also visible by eye, reverted [(POMCo)$_2$O] back to a Co^{II} species. Attempts to use electron energy loss spectroscopy (EELS),[20] Figure S6, also failed because of an insufficient signal-to-noise ratio for an analytical analysis. Magnetic susceptibility measurements, Figure S7, however, showed that [POMCo^{II}H$_2$O] is paramagnetic and [POMCo^{III}H$_2$O] is diamagnetic, while [(POMCo)$_2$O] showed a *significant* decrease in the magnetic susceptibility of 1 order of magnitude after correction to account for the presence of [POMCo^{II}H$_2$O] as an impurity and showed antiferromagnetic behavior. The low magnetic susceptibility may explain the chemical shifts and narrow lines observed in the ^{31}P NMR spectrum. [(POM-Co)$_2$O] is EPR silent down to 15 K in water, as expected for an antiferromagnetically coupled compound, although some impurity of [POMCo^{II}H$_2$O] can be observed at 15 K in the solid sample but not in solution.

Reactivity Studies. Since [(POMCo)$_2$O] is not stable in water and reverts back to [POMCo^{II}H$_2$O] as identified by ^{31}P NMR *but not to* [POMCo^{III}H$_2$O], it was reasonable to assume that water is oxidized to O$_2$. Indeed, we were able to measure by gas buret and analysis by gas chromatography the formation of 1 equivalent of O$_2$ per equivalent of [(POMCo)$_2$O], eq 1. This reaction stoichiometry also points toward the formulation of [(POMCo)$_2$O] as *formally* a bis-Co^{IV} compound since the formation of O$_2$ is necessarily a four-electron oxidation. See below for the more exact electronic structure analysis. A reaction where [(POMCo)$_2$O] was prepared in H$_2$^{18}O yielded ^{18}O$_2$ only. The cycle of formation of [(POMCo)$_2$O] from 10 mM [POMCo^{II}H$_2$O] and oxidation of water was repeated 10 times without any change in yield or rate of formation of O$_2$.

dx.doi.org/10.1021/ic402962c | *Inorg. Chem.* 2014, 53, 1779−1787

$$[(\alpha_2\text{-}P_2W_{17}O_{61}Co^{IV})_2O]^{14-} + 3H_2O \rightarrow 2[\alpha_2\text{-}P_2W_{17}O_{61}Co^{II}(H_2O)]^{8-} + O_2 + 2H^+ \quad (1)$$

A kinetic study of the water oxidation reaction *in dilute solutions* by the method of initial rates, Figure S8, carried out by measuring the optical density at 507 nm, the peak in the visible spectrum associated with $[(POMCo)_2O]$ (Figure 2), reveals that the reaction is indeed first-order in $[(POMCo)_2O]$. A first-order rate constant, $k_{obs} = 5.04 \times 10^{-5}$ s^{-1}, at 22 °C was calculated. Further study of the rate as a function of temperature, Figure S9, yielded measured activation energies, $\Delta H^{\ddagger}_{298} = 8.7$ kcal/mol, $\Delta S^{\ddagger}_{298} = -48.6$ cal/(mol K), and $\Delta G^{\ddagger}_{298} = 23.2$ kcal/mol. Reactions in D_2O showed no kinetic isotope effect.

The reactivity of $[(POMCo)_2O]$ was also assessed toward nucleophilic water-soluble organic compounds in oxygen transfer reactions. Thus, sulfonated triphenylphosphine, $P(PhSO_3^-Na^+)_3$, was quantitatively oxidized within seconds to the corresponding phosphine oxide, $P(O)(PhSO_3^-Na^+)_3$, in $P(PhSO_3^-Na^+)_3/[(POMCo)_2O]$ of 2 to 1, Scheme 1. Similarly dimethyl sulfoxide was quantitatively oxidized to the corresponding sulfone, Scheme 1.

Scheme 1. Oxidation of Water-Soluble Nucleophiles by $[(POMCo)_2O]$

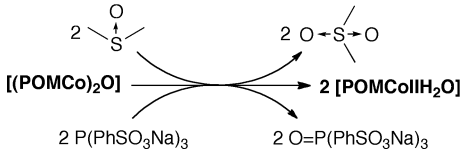

Interestingly, epoxidation of alkenes was not observed in a necessarily biphasic reaction; however in the presence of a slight excess of Mn^{III}tetramesityl porphyrin as an oxygen atom acceptor to form a competent epoxidizing intermediate, cyclooctene was oxidized within a few minutes to yield 2 equivalents of cyclooctene oxide per equivalent $[(POMCo)_2O]$, Scheme 2. Mn^{III}tetramesityl porphyrin does not

Scheme 2. Biphasic Epoxidation of Alkenes in the Presence of Mn^{III}(tetramesityl)porphyrin

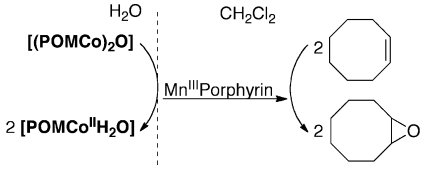

catalyze the epoxidation of cyclooctene with O_2; O_2 is not an intermediate in this reaction. When $[(POMCo)_2O]$ was prepared in $H_2{}^{18}O$, only 18-O labeled cyclooctene oxide was formed. All the aforementioned stoichiometric reactions support the conclusion that $[(POMCo)_2O]$ is a four-electron oxidant.

In reactions of water-soluble allylic alcohols with $[(POMCo)_2O]$, only C−H activation was observed with the chemoselective product formation of ketones or aldehydes. The propensity for C−H bond activation was tested on a series of water-soluble alcohols, Table 1. The general trend is quite clear. Oxidation is a function of the C−H bond dissociation energy (BDE), which is a strong indication that the oxidation

Table 1. Oxidation of Alcohols by $[(POMCo)_2O]^a$

substrate	product	yield, mol %	BDE, kJ/mol[27]
but-3-en-2-ol	but-3-en-2-one	65	unknown[b]
prop-2-en-1-ol	acrolein	52	341.1 ± 7.5
2-propanol	acetone	20	380.7 ± 4.2
ethanol	acetaldehyde	2	396.6 ± 4.2

[a]A solution of 5 mM $K[(POMCo)_2O]$and 40 mM substrate in D_2O was prepared at 0 °C and allowed to warm to RT. Products were quantified by ^1H and ^{31}P NMR. [b]The BDE of but-3-en-2-ol has not been reported, but the radical chlorination of but-3-en-2-ol is faster than that of allyl alcohol.[28].

proceeds either by a hydrogen atom transfer (HAT) mechanism or via formation of a metal alkoxide followed by rate-determining β-hydrogen elimination.[25] It should be noted that the chemical yields, especially for simple aliphatic alcohols, are low, likely due to competing water oxidation. This is most likely just a concentration effect since the concentration of water is ∼55 M versus only 40 mM alcohol. In fact, $[(POMCo)_2O]$ is quite a potent oxidant, capable even of catalytic but not stoichiometric oxidation of very difficult to oxidize fluoro-substituted alcohols such as trifluoroethanol, which has an *ab initio* calculated C−H BDE of 418 kJ/mol.[26] Thus, a solution of 5 mM $K[(POMCo)_2O]$ and 50 mM hexafluoroisopropanol in H_2O under a flow of ozone at ∼0 °C yielded 36 mol % hexafluoroacetone by ^{19}F NMR after 30 min.

The direct measurement of the reaction rates of the oxidation of methanol and ethanol in 10 vol % solutions in water is shown in Figure 6. Note that the reaction conditions are quite

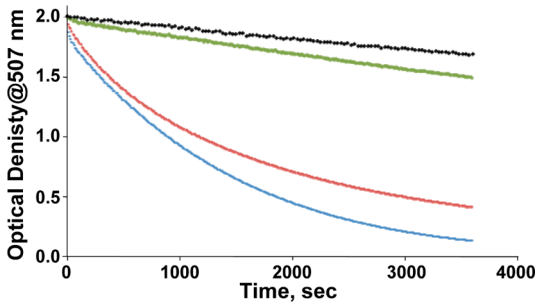

Figure 6. Kinetic profiles of the decay of a 0.15 mM aqueous $[(POMCo)_2O]$ solution at 22 °C. Black, H_2O only; blue, 10 vol % (1.71 M) ethanol; red, 10 vol % (2.47 M) methanol; green, 10 vol % (2.46 M) methanol-d_4. $k_{obs} = 4.41 \times 10^{-4}$ L/s (MeOH); $k_{obs} = 7.81 \times 10^{-5}$ L/s (MeOH-d_4); $k_{obs} = 5.04 \times 10^{-4}$ L/s (EtOH). $[POMCo^{II}H_2O]$ is completely inactive in all reactions.

different than those described in Table 1. The disappearance of $[(POMCo)_2O]$ species is faster in the presence of ethanol than methanol, as would be expected for the lower BDE of the reactive C−H bond in ethanol versus methanol. Both alcohols were oxidized much faster than water. Furthermore, a kinetic isotope effect for the oxidation of methanol was measured and yielded a $k_H/k_D = 5.65 \pm 0.2$. Both these kinetics measurements support a HAT or an alkoxide/β-hydrogen elimination mechanism.

Further support for the oxidation of alcohols by a HAT as opposed to an alkoxide/β-hydrogen elimination mechanism was obtained by reacting $K[(POMCo)_2O]$ with a spin trap, *N*-*tert*-butyl-α-phenylnitrone (PBN), Figure 7. In water only, a triplet spectrum ($A_N = 8.5$ G) was obtained. From the literature and based on the hyperfine coupling constants and computer

dx.doi.org/10.1021/ic402962c | Inorg. Chem. 2014, 53, 1779−1787

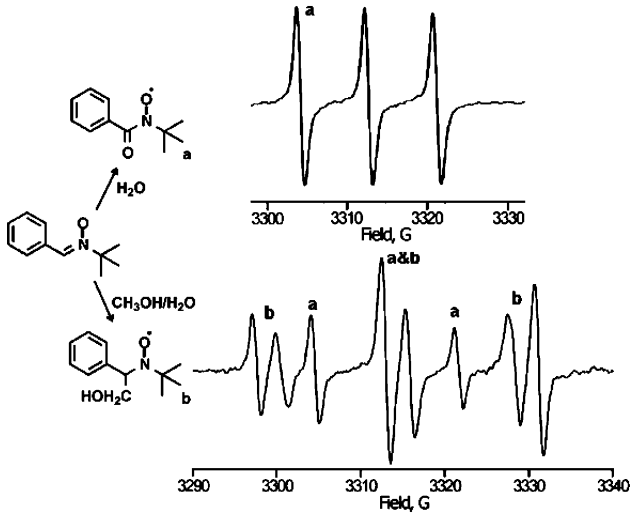

Figure 7. EPR spectra of spin adducts generated at 293 K from 5 mM $K[(POMCo)_2O]$ and 50 mM PBN in water (top) and in a 5.5 vol % CH_3OH/H_2O mixture (bottom). See Figure S11 for simulations.

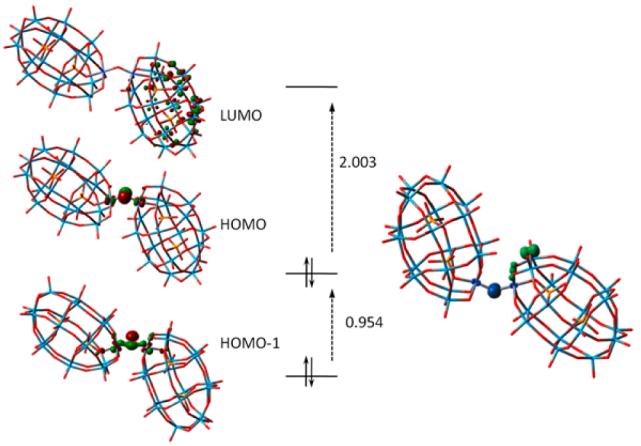

Figure 8. Molecular orbital diagram and spin density distributions. (Left) Orbital representations of the LUMO, HOMO, and HOMO−1 for the theoretical species $[(P_2W_{17}O_{61}Co^{III})_2O]^{16-}$ with energy gaps in eV. (Right) Computed ($\alpha-\beta$) spin density representation for the $[(\alpha_2\text{-}P_2W_{17}O_{61}Co^{IV})_2O]^{14-}$, $[(POMCo)_2O]$, species in the Ms = 0 broken symmetry state.

simulation the spin-adduct product was identified as PBNOx.[29] On the other hand in the same experiment in a 5.5 vol % CH_3OH/H_2O solution both the PBNOx and a new species (with a hextet spectrum; A_N = 15.1 G, A_H = 3.1 G) were observed. This spectrum is typical of spin adducts of PBN with $HOCH_2\bullet$, $CH_3O\bullet$, or $HO\bullet$ radicals, which are difficult to differentiate.[29] However, reaction in 5.5 vol % CD_3OH/H_2O showed almost exclusive formation of PBNOx, leading to the conclusion that the sextet observed in the EPR can be associated with the spin-adduct of PBN with $HOCH_2\bullet$ because of the higher BDE and thus less radical formation in CD_3OH versus that in CH_3OH.

Computational Analysis of the Electronic Structure. Computational methods have been extensively used to analyze the structure, electronic properties, and reactivity of polyoxometalates.[30] To characterize the electronic structure of the observed $[(POMCo)_2O]$ anion, DFT calculations using the B3LYP functional were performed on an experimentally prepared Wells−Dawson dimer with cobalt atoms in formal oxidations states III and IV ($[(P_2W_{17}O_{61}Co^{III})_2O]^{16-}$ and $[(P_2W_{17}O_{61}Co^{IV})_2O]^{14-}$). Full optimization was performed using the PCM approach to model the water solvent. The two polyoxometalate frameworks were arranged in a *trans* disposition to retain a symmetry plane. For $[(P_2W_{17}O_{61}Co^{III})_2O]^{16-}$, where there is no experimental analogue, the ground state is a singlet, as expected for a Co(III) in an octahedral environment. Importantly, the frontier orbitals display an electronic structure where the two highest occupied orbitals (HOMO and HOMO−1) are mainly localized on the Co−O−Co bridging unit and have a significant contribution of p-orbitals from the bridging oxygen and only a minor contribution of cobalt d-orbitals, Figure 8. The LUMO is centered on the polyoxometalate framework. This result is in line with the common axiom that it is difficult for cobalt ions to lose their fourth electron.

The calculation for $[(P_2W_{17}O_{61}Co^{IV})_2O]^{14-}$ or $[(POMCo)_2O]$ shows a reasonable fit of the $Co-O_{bridge}$ bond lengths (1.806 and 1.784 Å) compared to the experimental values of 1.79 and 1.77 Å. The calculated $Co-O_{bridge}-Co$ angle is, however, more acute, 139.1° versus the experimental values of 167°.[31] The first oxidation of $[(P_2W_{17}O_{61}Co^{III})_2O]^{16-}$ occurs on the bridging Co−O−Co oxygen as a consequence of the finding that the HOMO and HOMO−1 are mainly localized on the Co−O−Co bridging unit. The second electron, however, cannot be removed from the same oxygen atom, and therefore the electron spin density computed for two-electron-oxidizing $[(P_2W_{17}O_{61}Co)_2O]^{14-}$ in the Ms = 0 broken symmetry state shows the formation of cation radicals (holes) with one unpaired electron localized on the bridging oxygen and the other one localized on an oxygen atom in the polyoxometalate framework. A similar finding was also reported in another theoretical analysis where the description of an oxidized cobalt-oxo reactive species was described as a $Co^{III}O^{+\bullet}$ radical and not $Co^{IV}O$.[32] The singlet−triplet separation has been estimated to be about 30 cm^{-1}, showing a weak antiferromagnetic coupling of the unpaired electrons. Figure S12 shows the spin density computed for the triplet state.

Calculations based on a smaller Lindqvist-type polyoxometalate, $[(W_5O_{18}Co)_2O]^{q-}$, allows computations without symmetry restrictions. Overall, no significant differences were observed in the geometric and electronic structure of the Lindqvist derivative in comparison to the Wells−Dawson one, Figure S13. The fluxionality of the Co−O−Co bond and the bond angle in the dimer was also tested in order to evaluate if a change in the geometric structure could modify the electronic structure of $[(POMCo)_2O]$. A displacement of 0.5 Å of the bridging oxygen from its almost symmetrical optimal position toward one of the cobalt centers increases the energy by only 0.4 $kcal\cdot mol^{-1}$. Another displacement of 0.5 Å leads to a structure with the bridging oxygen forming two asymmetric bonds with bond distances of 1.750 and 1.866 Å, a structure that is 1.7 $kcal\cdot mol^{-1}$ above the optimal structure. The shortening of the bond does not modify, however, the $Co^{III}O^{+\bullet}$ *radical nature* of the bond. The potential influence of the Co−O−Co bond angle on the electronic structure of the dimer was also tested. When the Co−O−Co bond angle is changed from 170° to 130°, the energy changes only by 4 $kcal\cdot mol^{-1}$, and there is no significant effect on the electronic structure of the anion. To test for the fidelity of the computations, calculations were also carried out using the PBE0 functional, especially because it was reported that using the PBE0 functional the electronic structure of the cubane cluster

dx.doi.org/10.1021/ic402962c | *Inorg. Chem.* 2014, 53, 1779−1787

$[Co_4O_4(C_5H_5N)_4(CH_3CO_2)_4]^+$ can be described as a $Co^{IV}Co^{III}{}_3O_4$ species where the electron spin density is spread almost equally over the eight core atoms.[15c] In our dimer system, however, the spin density remains qualitatively unaltered using the PBE0 functional, Figure S14. Finally, we have carried out CASSCF calculations on the complete Lindqvist dimer anion using the geometry optimized at the DFT level. Multiconfigurational wave functions were constructed by distributing 14 electrons over 12 orbitals. The lowest root has precisely the same character as observed in the DFT calculations: one hole on the bridging oxygen and another hole localized on one of the oxygens of the Lindqvist cage, Figure S15. Among the 12 lowest CASSCF roots, there are no electronic states with extra holes on the Co ions.

CONCLUSIONS

An active species based on a cobalt-substituted Wells–Dawson polyoxometalate, $[(POMCo)_2O]$, has been isolated by oxidation of a known $[POMCo^{II}H_2O]$ compound with ozone. An, as yet, unproven pathway that would explain the formation of $[(POMCo)_2O]$ involves the oxidation of $[POMCo^{II}H_2O]$ with O_3, leading to a Co(III)-oxyl species that reacts with $[POMCo^{II}H_2O]$ to form a dimer, which is then oxidized by the excess O_3 in solution, Scheme 3. These oxo species are sufficiently labile in incorporating ^{18}O by fast exchange with $H_2{}^{18}O$.

Scheme 3. Suggested Pathway for the Formation of $[(POMCo)_2O]$

$$[POMCo^{II}\text{-}H_2O] + O_3 \longrightarrow [POMCo^{III}\text{-}O_3\bullet] \xrightarrow{-O_2} [POMCo^{III}\text{-}O\bullet]$$

$$[POMCo^{III}\text{-}O\bullet] \xrightarrow[O_3]{[POMCo^{II}\text{-}H_2O]} [(POMCo)_2O]$$

The X-ray diffraction measurements reveal an almost linear, 169.4(14)°, dicobalt-μ-oxo unit with an average Co–O bond length of 1.81 Å. The electronic structure as determined by DFT and CASSCF calculations indicates that $[(POMCo)_2O]$ is best represented as a compound with two cobalt(III) atoms and two oxygen cation radicals ($O^{+\bullet}$), one at the bridging oxygen atom and the other in the polyoxometalate framework. The representation of $[(POMCo)_2O]$ as a bis cobalt(IV) compound seems much less likely.

Solution phase ^{31}P NMR, UV–vis, and Raman spectroscopic studies of $[(POMCo)_2O]$ clearly differentiate $[(POMCo)_2O]$ from the $[POMCo^{II}H_2O]$ starting compound and the one-electron-oxidized analogue $[POMCo^{III}H_2O]$, which is stable in water and not reactive. On the other hand reactions of $[(POMCo)_2O]$ with H_2O, $P(PhSO_3Na)_3$, $CH_3S(O)CH_3$, and cyclooctene in the presence of a Mn(III) mesitylporphyrin yielded O_2, $P(O)(PhSO_3Na)_3$, $CH_3S(O)_2CH_3$, and cyclooctene oxide, respectively with coformation of $[POMCo^{II}H_2O]$, but not $[POMCo^{III}H_2O]$. The reaction stoichiometries in all these cases show that $[(POMCo)_2O]$ is a four-electron oxidant. Use of $H_2{}^{18}O$ as solvent leads to the formation almost exclusively of $^{18}O_2$- and 18-O-labeled oxygenates. The isotope labeling experiments indicate that oxygen atoms in $[(POMCo)_2O]$, at least those involved in water oxidation and oxygenation, quickly exchange with the solvent.[33] Although $[(POMCo)_2O]$ does not react directly with alkenes, it does activate C–H bonds of alcohols in water, where reactivity is a function of the bond dissociation energy. For methanol a kinetic isotope effect of 5.65 ± 0.2 was measured. In addition, EPR spectroscopy in the presence of spin adducts under methanol oxidation conditions shows the intermediacy of a $\bullet CH_2OH$ radical species. This spin-trapping experiments along with the reaction kinetics all point toward a hydrogen atom transfer mechanism for C–H bond activation.

The actual active species involved in the C–H bond activation and oxygen transfer reactions as well as the mechanism of water oxidation to O_2 remains unknown. The observation that the reaction is first-order in $[(POMCo)_2O]$ and that $[(POMCo)_2O]$ is a four-electron oxidant with 2 equivalents of $[POMCo^{II}H_2O]$ as products and no observed $[POMCo^{III}H_2O]$ intermediate suggests an intramolecular mechanism that likely includes addition of a water molecule to the bridge between the cobalt atoms, perhaps to form a bis-μ-hydroxy complex that rearranges to form O_2. This intermediate may likely also be involved in C–H bond activation and oxygen transfer reactions. The activation parameters for the water oxidation, $\Delta H^{\ddagger}_{298}$ = 8.7 kcal/mol, $\Delta S^{\ddagger}_{298}$ = −48.6 cal/(mol K), and $\Delta G^{\ddagger}_{298}$ = 23.2 kcal/mol, indicate a highly ordered transition state. It is notable that for methanol oxidation the activation parameters, $\Delta H^{\ddagger}_{298}$ = 6.9 kcal/mol, $\Delta S^{\ddagger}_{298}$ = −50.45 cal/(mol K), and $\Delta G^{\ddagger}_{298}$ = 21.95 kcal/mol, also indicate a highly ordered transition state for the alcohol oxidation reactions.

EXPERIMENTAL SECTION

Polyoxometalate Synthesis. The cobalt(II)-substituted Wells–Dawson polyoxometalate α_2-$K_8P_2Co(H_2O)W_{17}O_{61}\cdot 16H_2O$, K-$[POMCo^{II}H_2O]$, was synthesized according to the published procedure.[34] The cesium, Cs$[POMCo^{II}H_2O]$, and tetramethyl ammonium, TMA$[POMCo^{II}H_2O]$, salts were prepared by addition to a stirred solution of $[Co^{II}H_2O]$ in water (0.1 mmol, 10 mL) of 8.8 equivalents of CsCl or $(CH_3)_4NF$, respectively (0.88 mmol) in a minimum amount of water. The resulting suspension was stirred vigorously for 20 min, filtered, and recrystallized from hot water. The oxidized analogues Cs$[(POMCo)_2O]$ and TMA$[(POMCo)_2O]$ were isolated at 0 °C from the ozonated K$[POMCo^{II}H_2O]$ solution after purging of excess ozone via precipitation by the procedure described just above. The solids were separated by centrifugation, dried, and kept under an inert atmosphere at −80 °C. Very small single crystals suitable for X-ray analysis were obtained by precipitation with tetramethyl ammonium fluoride, followed by very fast recrystallization from a slightly warmed (~35 °C) aqueous solution. The diffraction data need to be collected as fast as possible after crystallization.

X-ray Structure Determination. Crystals were placed in Paratone oil (Hampton Research) and mounted on a MiTeGen cryoloop before being flash cooled in liquid nitrogen. Crystal data for compound $[(POMCo)_2O]$ were collected at 100 K using a Bruker Kappa ApexII CCD diffractometer with Mo Kα (λ = 0.71073 Å) radiation, graphite monochromator, and Miracol optics. The data were integrated with Bruker Apex2 Saint software. Routine Lorentz and polarization corrections were applied, and multiscan absorption corrections were performed using SADABS. Direct methods were performed using the program SHELXS-97. The tungsten and cobalt atoms were successfully located in the structure solution, and subsequent cycles of refinement using SHELXL-97 located the remaining atoms including tertiary methyl ammonium counterions. The refinements were weighted by full-matrix least-squares against $|F^2|$ using all data. In the final stages of refinement SQUEEZE was used due to the large voids and remaining disordered counterions and solvent molecules. In the refinement W and Co atoms were refined anisotropically, and oxygen and carbon atoms were refined isotropically due to the relatively low resolution of this structure, 0.9 Å. Hydrogen atoms were placed in calculated positions and refined in riding mode. Crystal data collection and refinement parameters are

dx.doi.org/10.1021/ic402962c | Inorg. Chem. 2014, 53, 1779–1787

given in Table 2, and the complete data can be found in the cif file as Supporting Information.

Table 2. Crystal Data and Structure Refinement for $[(POMCo)_2O]$[35]

empirical formula	$2(Co_{1.67}O_{123}P_4W_{34.33}),19(C_4H_{12}N),11(O)$
fw	9294.56
cryst syst	monoclinic
space group	$P2(1)/c$
a, Å	27.517(6)
b, Å	29.404(6)
c, Å	26.160(8)
α, deg	90.00
β, deg	112.306(9)
γ, deg	90.00
V, Å^3	19583(8)
Z	4
d_{calc}, mg/cm^3	3.153
μ, mm^{-1}	20.326
no. of reflns	86 029
no. of unique reflns	28 011
R_{int}	0.1490
R $[I > 2\sigma(I)]^a$	$R_1 = 0.0822$, $wR_2 = 0.1725$
goodness of fit	0.914

$^a R_1 = \sum||F_o| - |F_c||/\sum|F_o|$; $wR_2 = \{\sum[w(F_o^2 - F_c^2)^2]/\sum w(F_o^2)^2]\}^{1/2}$.

Oxidation of Organic Substrates. Oxidation reactions were typically carried out in 1 mL of 10 mM D_2O solutions of $K[POMCo^{II}H_2O]$, which was ozonated for 30 min at 0 °C and purged with argon. The amount of $K[(POMCo)_2O]$ was quantified by ^{31}P NMR, and then 4 equivalents of a substrate was added. The solution was left to heat slowly to room temperature with stirring. Products where identified and quantified by ^1H NMR using TMS as external standard. $Mn^{III}(TMP)Cl$ was prepared by metalation of tetramesitylporphyrin. A solution of $Mn^{III}(TMP)Cl$ (10 μmol) and cis-cyclooctene (50 μmol) in 1 mL of dichloromethane was added to 5 μmol of $[(POMCo)_2O]$ in 1 mL of water. The amount of cyclooctene oxide was determined by GC measurements using decane as external standard. 18-O-Labeled products were identified by GC-MS.

Oxidation of Water. The volume of O_2 was measured by direct methods, via connecting of the reaction vessel with a U-tube to a calibrated microburet with collection of the gas released. A 3 mL amount of a 12 mM $K[POMCo^{II}H_2O]$ solution was treated with ozone (concentration 25 mg/L, rate 6.25 mg/min) for 30 min and then purged/degassed with Ar to yield a 5 mM solution (by ^{31}P NMR) of $K[(POMCo)_2O]$. From this solution, which contains 15 μmol of $K[(POMCo)_2O]$, 0.33 mL of O_2 (13.5 μmol) was released at 20 °C (average over three experiments). The solubility of O_2 at 20 °C is 7.6 μg/mL, so 3 mL of water can optimally contain an additional 0.7 μmol of O_2. The O_2 yield can be estimated to be 95%.

Computational Details. All reported calculations were performed with the Gaussian09 package at the DFT level by means of the hybrid exchange−correlation B3LYP functional.[36] For P, Co, and W atoms, the LANL2DZ pseudopotential was used.[37] The 6-31G(d,p) basis set was used for O atoms directly bound to Co and the 6-31G basis set for the rest of the atoms.[38] All the structures were optimized in water solution using the IEF-PCM approach to model the solvent effects (ε = 78.36 and UFF radii).[39] Open shells were computed at the unrestricted DFT level. The Ms = 0 broken symmetry state for the 2e-oxidized species was determined using the broken symmetry approach at the geometry computed for the triplet state. For the sake of comparison spin density distributions were also determined with the hybrid PBE0 (Perdew−Burke−Ernzerhof exchange−correlation) functional.[40] CASSCF calculations were performed using MOLCAS[41] and with the same basis set as in the DFT calculations.

■ ASSOCIATED CONTENT

Ⓢ Supporting Information

More details on experimental and computational methods and additional spectroscopic, kinetic, and computational data. This material is available free of charge via the Internet at http://pubs.acs.org.

■ AUTHOR INFORMATION

Corresponding Author

*E-mail: Ronny.Neumann@weizmann.ac.il.

Notes

The authors declare no competing financial interest.

■ ACKNOWLEDGMENTS

This research was supported by the Israel Science Foundation grant no. 1073/10, the Helen and Martin Kimmel Center for Molecular Design, the Spanish Ministry of Science and Innovation (project no. CTQ2011-29054-C02-01), and the Generalitat de Catalunya (2009SGR462 and XRQTC). Gregory Lars Olsen is thanked for the MAS ^{31}P NMR measurements. R.N. is the Rebecca and Israel Sieff Professor of Chemistry.

■ REFERENCES

(1) Torres Pazmino, D. E.; Winkler, M.; Glieder, A.; Fraaije, M. W. *J. Biotechnol.* **2010**, *146*, 9−24.
(2) Messinger, J.; Noguchi, T.; Yano, J. *RSC Energy Environ. Ser.* **2012**, *5*, 163−207.
(3) Navarro, R. M.; Pena, M. A.; Fierro, J. L. G. *Chem. Ind.* **2006**, *108*, 463−490.
(4) Nocera, D. G. *Acc. Chem. Res.* **2012**, *45*, 767−776.
(5) Que, L., Jr.; Tolman, W. B. *Nature* **2008**, *455*, 333−340.
(6) (a) Liu, X.; Wang, F. *Coord. Chem. Rev.* **2012**, *256*, 1115−1136. (b) Du, P.; Eisenberg, R. *Energy Environ. Sci.* **2012**, *5*, 6012−6021. (c) McAlpin, J. G.; Stich, T. A.; Casey, W. H.; Britt, R. D. *Coord. Chem. Rev.* **2012**, *256*, 2445−2452. (d) Jiao, F.; Frei, H. *Energy Environ. Sci.* **2010**, *3*, 1018−1027.
(7) (a) Sheldon, R. A.; Kochi, J. K. *Metal-Catalyzed Oxidations of Organic Compounds*; Academic: New York, 1981. (b) *Oxygen Complexes and Oxygen Activation by Transition Metals*; Martell, A. E. Sawyer, D. T., Eds.; Plenum: New York, 1988. (c) Dioxygen Activation and Homogeneous Catalytic Oxidation. Simandi, L. I., Ed. *Stud. Surf. Sci. Catal.* **1991**, *66*, 1−696.
(8) (a) Koola, J. D.; Kochi, J. K. *J. Org. Chem.* **1987**, *52*, 4545−4553. (b) Zhang, X.; Sasaki, K.; Hill, C. L. *J. Am. Chem. Soc.* **1996**, *118*, 4809−4816.
(9) (a) Egan, J. W., Jr.; Haggerty, B. S.; Rheingold, A. L.; Sendlinger, S. C.; Theopold, K. H. *J. Am. Chem. Soc.* **1990**, *112*, 2445−2446. (b) Nam, I.; Kim, W.; Kim, Y.; Kim, C. *Chem. Commun.* **2001**, 1262−1263. (c) Song, Y. J.; Hyun, M. Y.; Lee, J. H.; Lee, H. G.; Kim, J. H.; Jang, S. P.; Noh, J. Y.; Kim, Y.; Kim, S.-J.; Lee, S. J.; Kim, C. *Chem.—Eur. J.* **2012**, *18*, 6094−6101.
(10) Pfaff, F. F.; Kundu, S.; Risch, M.; Pandian, S.; Heims, F.; Pryjomska-Ray, I.; Haack, P.; Metzinger, R.; Bill, E.; Dau, H.; Comba, P.; Ray, K. *Angew. Chem., Int. Ed.* **2011**, *50*, 1711−1715.
(11) Lacy, D. C.; Park, Y. J.; Ziller, J. W.; Yano, J.; Borovik, A. S. *J. Am. Chem. Soc.* **2012**, *134*, 17526−17535.
(12) (a) Brunschwig, B. S.; Chou, M. H.; Creutz, C.; Ghosh, P.; Sutin, N. *J. Am. Chem. Soc.* **1983**, *105*, 4832−4833. (b) Shafirovich, V. Ya.; Khannanov, N. K.; Strelets, V. V. *Nouv. J. Chim.* **1980**, *4*, 81−84.
(13) (a) Kanan, M. W.; Nocera, D. G. *Science* **2008**, *321*, 1072−1075. (b) Pijpers, J. J. H.; Winkler, M. T.; Surendranath, Y.; Buonassisi, T.; Nocera, D. G. *Proc. Natl. Acad. Sci. U.S.A.* **2011**, *108*, 10056−10061. (c) Surendranath, Y.; Lutterman, D. A; Liu, Y.; Nocera, D. G. *J. Am. Chem. Soc.* **2012**, *134*, 6326−6336. (d) Symes, M. D.; Surendranath, Y.; Lutterman, D. A.; Nocera, D. G. *J. Am. Chem. Soc.* **2011**, *133*,

5174−5177. (e) Kanan, M. W.; Yano, J.; Surendranath, Y.; Dinca, M.; Yachandra, V. K.; Nocera, D. G. *J. Am. Chem. Soc.* **2010**, *132*, 13692−13701.
(14) (a) Rigsby, M. L.; Mandal, S.; Nam, W.; Spencer, L. C.; Llobet, A.; Stahl, S. S. *Chem. Sci.* **2012**, *3*, 3058−3062. (b) Lai, W.; Cao, R.; Dong, G.; Shaik, S.; Yao, J.; Chen, H. *J. Phys. Chem. Lett.* **2012**, *3*, 2315−2319. (c) Leung, C.-F.; Ng, S.-M.; Ko, C.-C.; Man, W.-L.; Wu, J.; Chen, L.; Lau, T.-C. *Energy Environ. Sci.* **2012**, *5*, 7903−7907. (d) Hong, D.; Jung, J.; Park, J.; Yamada, Y.; Suenobu, T.; Lee, Y.-M.; Nam, W.; Fukuzumi, S. *Energy Environ. Sci.* **2012**, *5*, 7606−7616. (e) Wasylenko, D. J.; Palmer, R. D.; Schott, E.; Berlinguette, C. P. *Chem. Commun.* **2012**, *48*, 2107−2109. (f) Gerken, J. B.; McAlpin, J. G.; Chen, J. Y. C.; Rigsby, M. L.; Casey, W. H.; Britt, R. D.; Stahl, S. S. *J. Am. Chem. Soc.* **2011**, *133*, 14431−14442. (g) Luo, J.; Rath, N. P.; Mirica, L. M. *Inorg. Chem.* **2011**, *50*, 6152−6157. (h) Dogutan, D. K.; McGuire, R.; Nocera, D. G. *J. Am. Chem. Soc.* **2011**, *133*, 9178−9180. (i) Shevchenko, D.; Anderlund, M. F.; Thapper, A.; Styring, S. *Energy Environ. Sci.* **2011**, *4*, 1284−1287. (j) Ng, G. K-Y; Ziller, J. W.; Borovik, A. S. *Chem. Commun.* **2012**, *48*, 2546−2548.
(15) (a) Berardi, S.; La Ganga, G.; Natali, M.; Bazzan, I.; Puntoriero, F.; Sartorel, A.; Scandola, F.; Campagna, S.; Bonchio, M. *J. Am. Chem. Soc.* **2012**, *134*, 11104−11107. (b) La Ganga, G.; Puntoriero, F.; Campagna, S.; Bazzan, I.; Berardi, S.; Bonchio, M.; Sartorel, A.; Natali, M.; Scandola, F. *Faraday Discuss.* **2012**, *155*, 177−190. (c) McAlpin, J. G.; Stich, T. A.; Ohlin, C. A.; Surendranath, Y.; Nocera, D. G.; Casey, W. H.; Britt, R. D. *J. Am. Chem. Soc.* **2011**, *133*, 15444−15452. (d) McCool, N. S.; Robinson, D. M.; Sheats, J. E.; Dismukes, G. C. *J. Am. Chem. Soc.* **2011**, *133*, 11446−11449. (e) Symes, M. D.; Lutterman, D. A.; Teets, T. S.; Anderson, B. L.; Breen, J. J.; Nocera, D. G. *ChemSusChem* **2013**, *6*, 65−69.
(16) (a) Tueysuez, H.; Hwang, Yun J.; Khan, S. B.; Asiri, A. M.; Yang, P. *Nano Res.* **2013**, *6*, 47−54. (b) Grzelczak, M.; Zhang, J.; Pfrommer, J.; Hartmann, J.; Driess, M.; Antonietti, M.; Wang, X. *ACS Catal.* **2013**, *3*, 383−388. (c) Hu, X. L.; Piccinin, S.; Laio, A.; Fabris, S. *ACS Nano* **2012**, *6*, 10497−10504. (d) Yusuf, S.; Jiao, F. *ACS Catal.* **2012**, *2*, 2753−2760. (e) Jia, H.; Stark, J.; Zhou, L. Q.; Ling, C.; Sekito, T.; Markin, Z. *RSC Adv.* **2012**, *2*, 10874−10881. (f) Klahr, B.; Gimenez, S.; Fabregat-Santiago, F.; Bisquert, J.; Hamann, T. W. *J. Am. Chem. Soc.* **2012**, *134*, 16693−16700. (g) Ahn, H. S.; Tilley, T. D. *Adv. Funct. Mater.* **2013**, *23*, 227−233. (h) Zidki, T.; Zhang, L.; Shafirovich, V.; Lymar, S. V. *J. Am. Chem. Soc.* **2012**, *134*, 14275−14278. (i) Xi, L.; Tran, P. D.; Chiam, S. Y.; Bassi, P. S.; Mak, W. F.; Mulmudi, H. K.; Batabyal, S. K.; Barber, J.; Loo, J. S. C.; Wong, L. H. *J. Phys. Chem. C* **2012**, *116*, 13884−13889. (j) Liao, M.; Feng, J.; Luo, W.; Wang, Z.; Zhang, J.; Li, Z.; Yu, T.; Zou, Z. *Adv. Funct. Mater.* **2012**, *22*, 3066−3074. (k) Wang, Y.; Wang, Y.; Jiang, R.; Xu, R. *Ind. Eng. Chem. Res.* **2012**, *51*, 9945−9951. (l) Yamada, Y.; Yano, K.; Hong, D.; Fukuzumi, S. *Phys. Chem. Chem. Phys.* **2012**, *14*, 5753−5760. (m) Risch, M.; Shevchenko, D.; Anderlund, M. F.; Styring, S.; Heidkamp, J.; Lange, K. M.; Thapper, A.; Zaharieva, I. *Int. J. Hydrogen Energy* **2012**, *37*, 8878−8888. (n) Risch, M.; Klingan, K.; Ringleb, F.; Chernev, P.; Zaharieva, I.; Fischer, A.; Dau, H. *ChemSusChem* **2012**, *5*, 542−549. (o) Pilli, S. K.; Furtak, T. E.; Brown, L. D.; Deutsch, T. G.; Turner, J. A.; Herring, A. M. *Energy Environ. Sci.* **2011**, *4*, 5028−5034. (p) Jeon, T. H.; Choi, W.; Park, H. *Phys. Chem. Chem. Phys.* **2011**, *13*, 21392−21401. (q) Chou, N. H.; Ross, P. N.; Bell, A. T.; Tilley, T. D. *ChemSusChem* **2011**, *4*, 1566−1569. (r) Wee, T.-L.; Sherman, B. D.; Gust, D.; Moore, A. L.; Moore, T. A.; Liu, Y.; Scaiano, J. C. *J. Am. Chem. Soc.* **2011**, *133*, 16742−16745. (s) Barroso, M.; Cowan, A. J.; Pendlebury, S. R.; Gratzel, M.; Klug, D. R.; Durrant, J. R. *J. Am. Chem. Soc.* **2011**, *133*, 14868−14871. (t) Young, E. R.; Costi, R.; Paydavosi, S.; Nocera, D. G.; Bulovic, V. *Energy Environ. Sci.* **2011**, *4*, 2058−2061. (u) Zhong, D. K.; Cornuz, M.; Sivula, K.; Gratzel, M.; Gamelin, D. R. *Energy Environ. Sci.* **2011**, *4*, 1759−1764. (v) Young, E. R.; Nocera, D. G.; Bulovic, V. *Energy Environ. Sci.* **2010**, *3*, 1726−1728. (w) Risch, M.; Khare, V.; Zaharieva, I.; Gerencser, L.; Chernev, P.; Dau, H. *J. Am. Chem. Soc.* **2009**, *131*, 6936−6937. (x) Zhong, D. K.; Gamelin, D. R. *J. Am. Chem. Soc.* **2010**, *132*, 4202−4207.
(17) (a) Yin, Q.; Tan, J. M.; Besson, C.; Geletii, Y. V.; Musaev, D. G.; Kuznetsov, A. E.; Luo, Z.; Hardcastle, K. I.; Hill, C. L. *Science* **2010**, *328*, 342−345. (b) Huang, Z.; Luo, Z.; Geletii, Y. V.; Vickers, J. W.; Yin, Q.; Wu, D.; Hou, Y.; Ding, Y.; Song, J.; Musaev, D. G.; Lian, T.; Hill, C. L. *J. Am. Chem. Soc.* **2011**, *133*, 2068−2071. (c) Huang, Z.; Geletii, Y. V.; Musaev, D. G.; Hill, C. L.; Lian, T. *Ind. Eng. Chem. Res.* **2012**, *51*, 11850−11859. (d) Zhu, G.; Geletii, Y. V.; Koegerler, P.; Schilder, H.; Song, J.; Lense, S.; Zhao, C.; Hardcastle, K. I.; Musaev, D. G.; Hill, C. L. *Dalton Trans.* **2012**, *41*, 2084−2090. (e) Goberna-Ferron, S.; Vigara, L.; Soriano-Lopez, J.; Galan-Mascaros, J. R. *Inorg. Chem.* **2012**, *51*, 11707−11715. (f) Tanaka, S.; Annaka, M.; Sakai, K. *Chem. Commun.* **2012**, *48*, 1653−1655. (g) Wu, J.; Liao, L.; Yan, W.; Xue, Y.; Sun, Y.; Yan, X.; Chen, Y.; Xie, Y. *ChemSusChem* **2012**, *5*, 1207−1212.
(18) (a) Stracke, J. J.; Finke, R. G. *J. Am. Chem. Soc.* **2011**, *133*, 14872−14875. (b) Natali, M.; Berardi, S.; Sartorel, A.; Bonchio, M.; Campagna, S.; Scandola, F. *Chem. Commun.* **2012**, *48*, 8808−8810. (c) Lieb, D.; Zahl, A.; Wilson, E. F.; Streb, C.; Nye, L. C.; Meyer, K.; Ivanovic-Burmazovic, I. *Inorg. Chem.* **2011**, *50*, 9053−9058.
(19) (a) Lv, H.; Geletii, Y. V.; Zhao, C.; Vickers, J. W.; Zhu, G.; Luo, Z.; Song, J.; Lian, T.; Musaev, D. G.; Hill, C. L. *Chem. Soc. Rev.* **2012**, *41*, 7572−7589. (b) Mizuno, N.; Kamata, K.; Yamaguchi, K. *Top. Organomet. Chem.* **2011**, *37*, 127−160.
(20) Barats, D.; Leitus, G.; Popovitz-Biro, R.; Shimon, L. J. W.; Neumann, R. *Angew. Chem., Int. Ed.* **2008**, *47*, 9908−9912.
(21) Pestovsky, O.; Stoian, S.; Bominaar, E. L.; Shan, X.; Münck, E.; Que, L., Jr.; Bakac, A. *Angew. Chem., Int. Ed.* **2005**, *44*, 6871−6874.
(22) Neumann, R.; Khenkin, A. M. *Chem. Commun.* **1998**, 1967−1968.
(23) (a) Jorris, T. L.; Kozik, M.; Casan-Pastor, N.; Domaille, P. J.; Finke, R. G.; Miller, W. K.; Baker, L. C. W *J. Am. Chem. Soc.* **1987**, *109*, 7402−7408. (b) Khenkin, A. M.; Kumar, D.; Shaik, S.; Neumann, R. *J. Am. Chem. Soc.* **2006**, *128*, 15451−15460.
(24) Sanders-Loehr, J.; Wheeler, W. D.; Shiemke, A. K.; Averill, B. A.; Loehr, T. M. *J. Am. Chem. Soc.* **1989**, *111*, 8084−8093.
(25) Mayer, J. M. *Acc. Chem. Res.* **2011**, *44*, 36−48.
(26) Song, K.-S.; Liu, L.; Guo, Q.-X. *Tetrahedron* **2004**, *60*, 9909−9923.
(27) Luo, Y.-R. *Handbook of Bond Dissociation Energies in Organic Compounds*; CRC Press: Boca Raton, 2003.
(28) Takahashi, K.; Xing, J.-H.; Hurley, M. D.; Wallington, T. J. *J. Phys. Chem. A* **2010**, *114*, 4224−4231.
(29) Buettner, G. R. *Free Radical Biol. Med.* **1987**, *3*, 259−303.
(30) Lopez, X.; Carbo, J. J.; Bo, C.; Poblet, J. M. *Chem. Soc. Rev.* **2012**, *41*, 7537−7571.
(31) The discrepancy between the experimental and calculated Co−O−-Co bond angles precludes the meaningful calculation of the expected Raman frequencies, since they are strongly a function of the bond angle.
(32) Wang, L.-P.; Van Voorhis, T. *J. Phys. Chem. Lett.* **2011**, *2*, 2200−2204.
(33) This is known also for other dicobalt-μ-oxo compounds; cf. Larsen, P. L.; Parolin, T. J.; Powell, D. R.; Hendrich, M. P.; Borovik, A. S. *Angew. Chem., Int. Ed.* **2003**, *42*, 85−89.
(34) Lyon, D. K.; Miller, W. K.; Novet, T.; Domaille, P. D.; Evitt, E.; Johnson, D. C.; Finke, R. G. *J. Am. Chem. Soc.* **1991**, *113*, 7209−7221.
(35) The disorder in the location of the countercations reduces the resolution and R_{int}. This is not unusual even for stable structures of polyoxometalates; cf. Ibrahim, M.; Xiang, Y.; Bassil, B. S.; Lan, Y.; Powell, A. K.; de Oliveira, P.; Keita, B.; Kortz, U. *Inorg. Chem.* **2013**, 8399−8408.
(36) (a) Lee, C.; Yang, C.; Parr, R. G. *Phys. Rev. B* **1988**, *37*, 785−789. (b) Becke, A. D. *J. Chem. Phys.* **1993**, *98*, 5648−5652. (c) Stephens, P. J.; Devlin, F. J.; Chabalowski, C. F.; Frisch, M. J. *J. Phys. Chem.* **1994**, *98*, 11623−11627.
(37) Hay, P. J.; Wadt, W. R. *J. Chem. Phys.* **1985**, *82*, 270−283.
(38) (a) Francl, M. M.; Pietro, W. J.; Hehre, W. J.; Binkley, J. S.; Gordon, M. S.; Defrees, D. J.; Pople, J. A. *J. Chem. Phys.* **1982**, *77*, 3654−3665. (b) Hehre, W. J.; Ditchfield, R.; Pople, J. A. *J. Chem. Phys.*

1972, *56*, 2257−2261. (c) Hariharan, P. C.; Pople, J. A. *Theor. Chim. Acta* **1973**, *28*, 213−222.
(39) Cances, E.; Mennucci, B.; Tomasi, J. *J. Chem. Phys.* **1997**, *107*, 3032−3041.
(40) (a) Perdew, J. P.; Burke, K.; Ernzerhof, M. *Phys. Rev. Lett.* **1996**, *77*, 3865−3868. (b) Adamo, C.; Barone, V. *J. Chem. Phys.* **1999**, *110*, 6158−6169.
(41) Aquilante, F.; De Vico, L.; Ferré, N.; Ghigo, G.; Malmqvist, P.-Å.; Neograd y, P.; Pedersen, T. B.; Pitonak, M.; Reiher, M.; Roos, B. O.; Serrano-Andrés, L.; Urban, M.; Veryazov, V.; Lindh, R. *J. Comput. Chem.* **2010**, *31*, 224−247.

dx.doi.org/10.1021/ic402962c | *Inorg. Chem.* 2014, 53, 1779−1787